Impact of Chromatic and Polarization-Mode Dispersions on DPSK Systems Using Interferometric Demodulation and Direct Detection

Jin Wang, *Student Member, IEEE,* and Joseph M. Kahn, *Fellow, IEEE*

***Abstract*—We study the impact of chromatic dispersion (CD) and first-order polarization-mode dispersion (PMD) on systems using binary differential phase-shift keying (2-DPSK) or quaternary DPSK (4-DPSK) with nonreturn-to-zero (NRZ) or return-to-zero (RZ) formats. These signals are received using optical preamplification, interferometric demodulation, and direct detection. We consider the linear propagation regime and compute optical power penalties at fixed bit-error ratio (BER). In order to evaluate the BER precisely taking account amplifier noise, arbitrary pulse shapes, arbitrary optical and electrical filtering, CD, and PMD, we introduce a novel model for DPSK systems and compute the BER using a method recently proposed by Forestieri for ON–OFF keying (OOK) systems. We show that when properly applied, the method yields highly accurate results for DPSK systems. We have found that when either the NRZ or RZ format is used, 2-DPSK exhibits lower power penalties than OOK in the presence of CD and first-order PMD. RZ-2-DPSK, as compared with NRZ-2-DPSK, incurs smaller penalties due to PMD, but offers no advantage in terms of CD. 4-DPSK, as it has twice the symbol duration of OOK or 2-DPSK for a given bit rate, incurs much lower CD and PMD power penalties than either of these techniques. RZ-4-DPSK is especially promising, as it offers CD and PMD penalties significantly smaller than all other techniques, including NRZ-4-DPSK.**

***Index Terms*—Direct detection, differential phase-shift keying (DPSK), interferometric demodulation, optical fiber communication, optical fiber dispersion, optical noise, polarization-mode dispersion (PMD).**

I. Introduction

ALTHOUGH most optical fiber communication systems currently use binary ON–OFF keying (OOK), high-capacity, long-haul transmission experiments using binary differential phase-shift keying (2-DPSK) and quaternary DPSK (4-DPSK) with nonreturn-to-zero (NRZ) and return-to-zero (RZ) formats have been reported by several groups in recent years [1]–[6]. These experiments have used Mach–Zehnder interferometers (MZIs) to convert received DPSK signals to intensity-modulated signals, enabling the use of direct-detection receivers. In optically amplified systems, for a given bit-error ratio (BER), 2-DPSK requires nearly 3 dB lower optical signal-to-noise ratio (OSNR) than OOK, enabling extended reach. 4-DPSK offers all the advantages of multilevel encoding—increased spectral efficiency, improved tolerance to chromatic dispersion (CD) and polarization-mode dispersion (PMD), and relaxed component bandwidth requirements—without incurring a power penalty with respect to OOK.

Experimental demonstrations have outpaced theoretical performance analysis of DPSK systems, especially in relation to the impact of CD and PMD. Reference [7] analyzed NRZ-2-DPSK systems under CD but quantified degradation in terms of eye penalty, as opposed to the more relevant performance measure of power penalty. Reference [8] studied the impact of CD and PMD on amplitude-shift keying and DPSK with coherent detection but obtained PMD penalties that seem unrealistically high for both modulation formats. The dearth of analysis of DPSK systems seems to arise mainly because of the difficulty of characterizing the probability distribution of decision variables and evaluating the BER in DPSK systems when intersymbol interference (ISI) arises from optical and electrical filtering and from dispersion. The BER performance of optically amplified DPSK systems with interferometric direct-detection receivers has been analyzed in [9] and [10], but the method used in [9] does not fully characterize the distribution of decision variables, while the method of [10] is too complicated for the study of dispersion effects.

Recently, Forestieri has proposed a computationally efficient method to analytically evaluate the BER in optically preamplified OOK systems [11], taking account of ASE, pulse shaping, optical and electrical filtering, and CD. This method employs a KLSE to describe the optical noise and, in this respect, is quite similar to early methods used to analyze square-law detectors [12], [13]. In this paper, we show that such a method is also applicable to DPSK systems using interferometric demodulation and direct detection and yields very accurate results. We employ this method to calculate the BERs of 2-DPSK and 4-DPSK with NRZ and RZ formats in the presence of CD and first-order PMD, and we evaluate the power penalties caused by these dispersion effects. We note that other methods have been used to compute BERs in optical preamplified OOK systems [14], [15]. These techniques can be adapted to DPSK systems as well, as in [16]. Nonetheless, the present paper is the first to present full details of a BER calculation technique for DPSK and to verify the technique using Monte Carlo simulation.

The remainder of this paper is organized as follows. In Section II, we describe the model used for 2-DPSK and 4-DPSK systems in the presence of CD and PMD. In Section III, we

Manuscript received December 4, 2002; revised September 22, 2003.

J. Wang is with the Department of Electrical Engineering and Computer Science, University of California, Berkeley, Berkeley, CA 94720 USA (e-mail: wangjin@eecs.berkeley.edu).

J. M. Kahn is with the Department of Electrical Engineering, Stanford University, Stanford, CA 94305 USA (e-mail: jmk@ee.stanford.edu).

Digital Object Identifier 10.1109/JLT.2003.822101

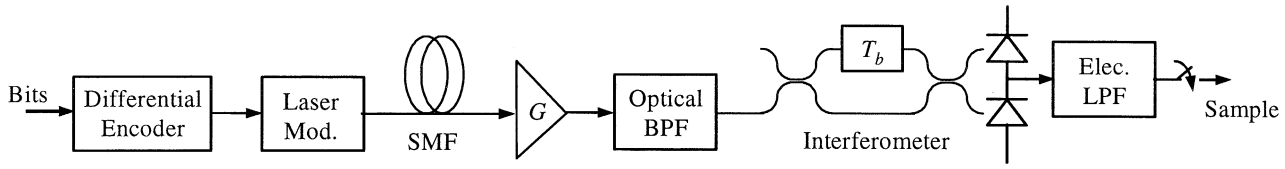

Fig. 1. Schematic of 2-DPSK system with optical preamplifier, delay-line interferometer, and balanced direct-detection receiver.

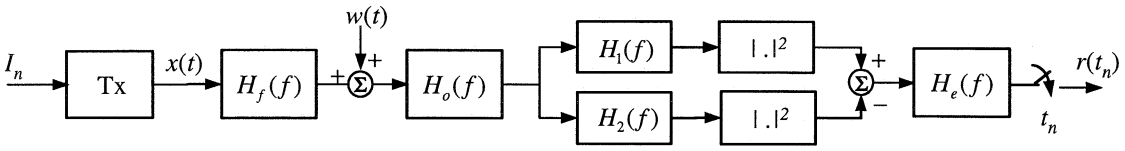

Fig. 2. Low-pass equivalent 2-DPSK system in the absence of PMD, assuming that a polarizer (aligned with the received signal) is inserted just before or after the optical bandpass filter.

discuss how to apply the KLSE method to compute BERs for these systems. In Section IV, we present power penalties caused by CD and PMD in DPSK systems. We present conclusions in Section V.

II. Transmission System Modeling

A. 2-DPSK Systems

A 2-DPSK system is represented schematically in Fig. 1. Each transmitted symbol conveys 1 bit, which is encoded in $\Delta\phi$, the phase difference between successive symbols, where $\Delta\phi \in \{0, \pi\}$. The optical source is assumed to be a single-frequency laser whose linewidth is negligible in comparison to the symbol rate, so that laser phase noise is negligible. External modulation is used to modulate the DPSK optical signal, as specified in detail hereafter. The optical signal is launched into a SMF operating in the linear regime (fiber nonlinearities are neglected throughout this paper). In the fiber, the optical signal is affected by CD and PMD.

The received optical signal passes into a lumped optical amplifier, which adds ASE noise. The amplifier output is filtered by an optical bandpass filter and is passed into an optical delay-line (Mach–Zehnder) interferometer, which demodulates the received DPSK signal. We assume that the interferometer's two branches are correctly phased so that its outputs yield, respectively, the sum and difference of the received field and the received field delayed by one symbol interval. A balanced optical receiver yields a photocurrent proportional to the difference between the intensities at the two interferometer output ports. This photocurrent is low-pass-filtered and sampled, and binary decisions are performed.

Fig. 2 shows the low-pass equivalent model for a DPSK system for the special case that PMD is absent and a polarizer (aligned with the signal) is placed just before or after the optical bandpass filter to remove the ASE component that is polarized orthogonal to the signal. For the sake of clarity, we will first develop a mathematical model for the system of Fig. 2 and then use the results to build up a more complicated model that describes a realistic system, which does not use a polarizer and in which PMD may be present.

In Fig. 2, $x(t)$ is the baseband equivalent representation of the signal field at the fiber input which, for either 2-DPSK or 4-DPSK, can be expressed in the form

$$x(t) = \sum_n I_n p(t - nMT_b). \tag{1}$$

The symbol sequence is represented by $\{I_n\}$ where, in a 2-DPSK system, $I_n \in \{e^{j0}, e^{j\pi}\}$. The bit duration is T_b, and the symbol duration is MT_b, where M =1, 2 for 2-DPSK and 4-DPSK, respectively. The elementary pulse shape is represented by $p(t)$. In this paper, we assume $p(t)$ is given by

$$p(t) = \begin{cases} \sqrt{\frac{E_b}{T_b}} & \text{NRZ-DPSK} \\ \sqrt{\frac{2E_b}{T_b}} \cos\left(\frac{\pi}{2}\cos^2\left(\frac{\pi t}{MT_b}\right)\right) & \text{RZ-DPSK} \end{cases} \tag{2}$$

within the symbol interval $[0, MT_b)$, and zero outside this interval. In (2), E_b denotes the optical energy per transmitted bit. Note that for NRZ-DPSK, $p(t)$ is simply a rectangular pulse,[1] while for RZ-DPSK, $p(t)$ corresponds to the output of a MZM driven by a sinusoidal clock at the symbol rate $1/MT_b$ [5]. We note that the signal model given by (1) corresponds to that used by Forestieri in [11], but the BER calculation method used in [11] and in this paper does not require the signal to be modeled in the form of (1). Rather, this method is applicable so long as we know how to describe the Fourier spectrum of $x(t)$.

In Fig. 2, $H_f(f)$ is the transfer function of a lossless fiber. When PMD is absent and only CD is considered, we can express the transfer function of the fiber as [7]

$$H_f(f) = \exp(-j2\pi^2\beta_2 L f^2) \tag{3}$$

where $\beta_2 \equiv -(D(\lambda)\lambda^2/(2\pi c)$, $D(\lambda)$ is the fiber CD parameter, L is the fiber length, and λ is the wavelength. At a wavelength

[1]We have also performed calculations using more realistic NRZ optical signals produced by a Mach–Zehnder modulator (MZM). The modulator electrical drive signal is a rectangular-pulse NRZ signal that has been passed through a fifth-order Bessel filter having bandwidth $0.85/MT_b$. For these more realistic NRZ optical signals, the mathematical description of the signal and the computation technique become more complicated, but CD penalties are only very slightly smaller than those for rectangular NRZ optical pulses.

$\lambda = 1.55$ μm in standard SMF, $D(\lambda)$ is typically of the order of 17 ps/nm/km.

The optical preamplifier in Fig. 2 is assumed to have flat gain G. We model the ASE noise as additive white Gaussian noise (AWGN) with one-sided power spectral density $n_{\rm sp}(G-1)h\nu$ in each polarization, where $n_{\rm sp} \geq 1$ is the spontaneous emission parameter and $h\nu$ is the photon energy [11]. We assume that the gain G is sufficiently high that ASE dominates over shot noise and thermal noise in the receiver, allowing us to ignore the latter two noises. In Fig. 2, $w(t)$ represents the ASE noise as complex circular AWGN with two-sided power spectral density $N_0 = n_{\rm sp}h\nu(G-1)/(G)$. We assume that $G \gg 1$ so that $N_0 \approx n_{\rm sp}h\nu$. We have assumed the fiber is lossless, which implies that the average received energy per bit will be equal to the transmitted energy per bit E_b.

In Fig. 2, $H_o(f)$ represents the equivalent low-pass transfer function of the optical bandpass filter. In this paper, the optical filter is either a Fabry-Pérot (FP) filter or a fiber Bragg grating (FBG) filter. For an FP filter, $H_o(f)$ is given under the Lorentzian approximation as [17]

$$H_o(f) = \frac{1}{\left(1 + \frac{j2f}{B_o}\right)} \tag{4}$$

where B_o is the 3-dB bandwidth (full-width at half-maximum) of the optical filter. For an FBG filter, we have [18]

$$H_o(f) = \frac{1}{\tanh(\kappa L_g)} \cdot \frac{j\kappa \sin\left[\beta(f)L_g\right]}{\beta(f)\cos\left[\beta(f)L_g\right] - j2\pi\left(\frac{f}{\nu_g}\right)\sin\left[\beta(f)L_g\right]} \tag{5}$$

where $\beta(f) = \sqrt{(2\pi f/\nu_g)^2 - \kappa^2}$, κ is the grating coupling coefficient, and L_g is the grating length. We assume typical values $\kappa = 6$ cm^{-1} and $\kappa L_g = 2$, and adjust ν_g to obtain the desired bandwidth.

After the bandpass filter in Fig. 2, $H_1(f)$ and $H_2(f)$ represent the transfer functions of the delay-line interferometer from its input port to its sum and difference ports, respectively. For the interferometer shown in Fig. 1, in which one branch has a delay equal to the bit duration T_b, we have

$$H_1(f) = \frac{[\exp(-j2\pi fT_b) + 1)]}{2}$$
$$H_2(f) = \frac{[\exp(-j2\pi fT_b) - 1)]}{2}. \tag{6}$$

In Fig. 2, $H_e(f)$ represents the transfer function of the electrical low-pass filter, which is always assumed to be a fifth-order Bessel type with transfer function [19]

$$H_e(f) = \frac{945}{jF^5 + 15F^4 - 105jF^3 - 420F^2 + 945jF + 945} \tag{7}$$

where $F = 2.43f/B_e$, and B_e is the 3-dB cutoff frequency. In this paper, both B_o and B_e are specified in terms of the bit rate R, which is the reciprocal of the bit duration T_b, i.e., $R = (1/T_b)$. In Fig. 2, the low-pass filter output $r(t)$ is sampled at the symbol rate to obtain the decision variable sequence $r(t_n)$.

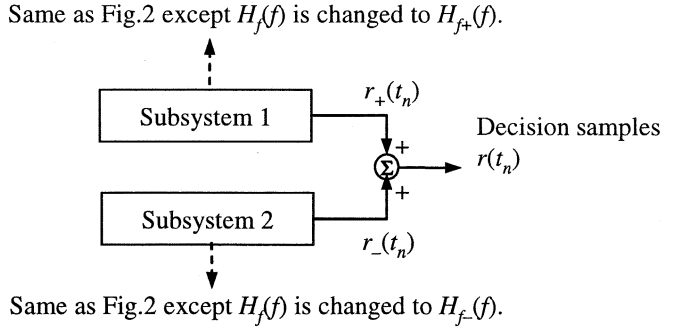

Fig. 3. Low-pass equivalent 2-DPSK system when PMD is present and no polarizer is used.

We now consider first-order PMD effects. We assume that there is negligible polarization-dependent loss so that we can use the principal states model [20] to characterize first-order PMD. Under this model, there exist a pair of orthorgonal input principal states of polarization (PSPs) $\hat{\varepsilon}_{a+}$ and $\hat{\varepsilon}_{a-}$, and a pair of orthorgonal output PSPs $\hat{\varepsilon}_{b+}$ and $\hat{\varepsilon}_{b-}$, where all of the PSPs are expressed as Jones vectors. If an arbitrarily polarized field $\vec{E}_a(t) = E_a(t)\hat{\varepsilon}_a$ is input to the fiber, this input field can be projected onto the two input PSPs [21] as

$$\vec{E}_a(t) = \sqrt{\gamma}E_a(t)\hat{\varepsilon}_a + \sqrt{1-\gamma}E_a(t)\hat{\varepsilon}_{a-} \tag{8}$$

where γ is the PMD power-splitting ratio, given by $\gamma = [\hat{\varepsilon}_a^{\dagger} \cdot \hat{\varepsilon}_{a+}]^2$. In terms of first-order PMD, the output field of the fiber takes the form [21], [22]

$$\vec{E}_b(t) = \sqrt{\gamma}E_a\left(t - \tau_0 - \frac{\Delta\tau}{2}\right)\hat{\varepsilon}_b + \sqrt{1-\gamma}E_a\left(t - \tau_0 + \frac{\Delta\tau}{2}\right)\hat{\varepsilon}_{b-} \tag{9}$$

where τ_0 is the polarization-independent group delay, and $\Delta\tau$ is the differential group delay (DGD) between the two PSPs. According to (9), the fiber transfer function for first-order PMD is given by

$$H_f(f) = \sqrt{\gamma}\exp\left[j2\pi f\left(\frac{-\Delta\tau}{2}\right)\right]\hat{\varepsilon}_{b+} + \sqrt{1-\gamma}\exp\left[j2\pi f\left(\frac{\Delta\tau}{2}\right)\right]\hat{\varepsilon}_{b-} \tag{10}$$

where we have neglected the polarization-independent group delay τ_0. Taking account of both CD and first-order PMD, we combine (3) and (10) to obtain the fiber transfer function

$$H_f(f) = H_{f+}(f)\hat{\varepsilon}_{b+} + H_{f-}(f)\hat{\varepsilon}_{b-}$$
$$H_{f+}(f) = \sqrt{\gamma}\exp\left[j2\pi f\left(\frac{-\Delta\tau}{2}\right) - j2\pi^2\beta_2 Lf^2\right]$$
$$H_{f-}(f) = \sqrt{1-\gamma}\exp\left[j2\pi f\left(\frac{\Delta\tau}{2}\right) - j2\pi^2\beta_2 Lf^2\right]. \tag{11}$$

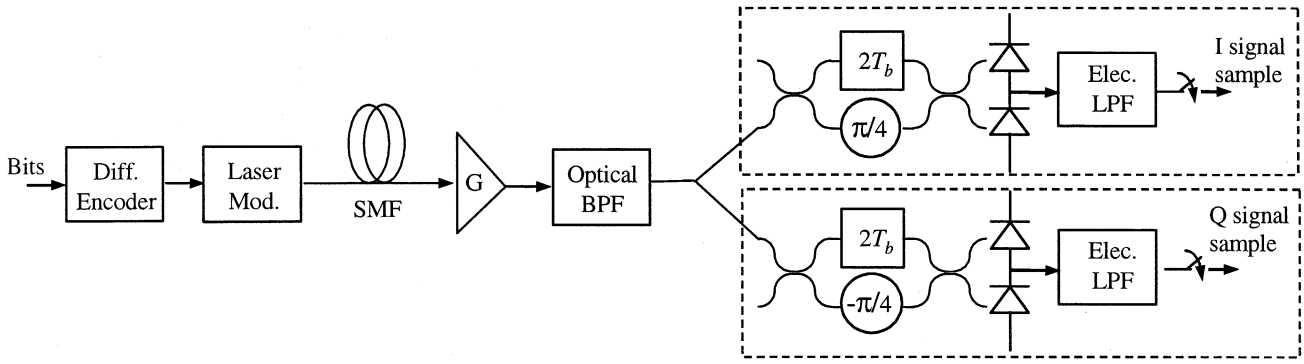

Fig. 4. Schematic of 4-DPSK system with optical preamplifier, delay-line interferometers, and balanced direct-detection receivers.

As suggested in (10) and (11), one can consider that the signal components in the two output PSPs propagate independently through the fiber and, indeed, that they propagate independently through the entire system from the modulator to the balanced receiver. At the receiver, the fields corresponding to the two PSPs are separately squared, and the resulting photocurrents are summed. From this perspective, we can decompose the entire system into a pair of subsystems, each corresponding to one PSP. Hence, we model the system as shown in Fig. 3. In Fig. 3, the upper system is modeled exactly like Fig. 2, except we replace $H_f(f)$ by $H_{f+}(f)$ and obtain sampled decision variables $r_+(t_n)$. Likewise, the lower system corresponds to Fig. 2, with $H_f(f)$ replaced by $H_{f-}(f)$, and with sampled decision variables $r_-(t_n)$. At the output of Fig. 3, we sum the outputs of the two subsystems to obtain sampled decision variables $r(t_n) = r_+(t_n) + r_-(t_n)$. Note that the ASE components of $r_+(t_n)$ and $r_-(t_n)$ are statistically independent. In what follows, we refer to the model in Fig. 3 as the "two-PSP" model and use it in the CD and PMD power-penalty computations. Although we consider only first-order PMD in computing the PMD power penalty, according to [23], our analysis is a reasonable approximation to the power penalty considering all orders of PMD.

B. 4-DPSK Systems

The modeling of a 4-DPSK system is similar to that of a 2-DPSK system, so we will only describe the differences here. A 4-DPSK system is represented schematically in Fig. 4. The baseband equivalent electric field at the fiber input $x(t)$ is described by (1) with pulse shape $p(t)$ given by (2) and with $M = 2$. Thus, the symbol duration is twice the bit duration, i.e., $2T_b$. Each transmitted symbol conveys two bits, encoded in four possible phase differences between successive symbols $\Delta\phi \in \{0, \pi/2, \pi, 3\pi/2\}$. Hence, $I_n \in \{e^{j0}, e^{j\pi/2}, e^{j\pi}, e^{j3\pi/2}\}$.

At the receiving end, two sets of interferometers, balanced receivers, low-pass filters, and samplers are used to demodulate and detect the in-phase (I) and quadrature (Q) components of the signal. In each interferometer, the upper branch has a delay equal to the symbol duration $2T_b$. In the I interferometer, the lower branch has an excess phase shift of $\pi/4$ so that the transfer functions to the sum and difference output ports are

$$H_{1I}(f) = \frac{\left[\exp(-j4\pi f T_b) + \exp\left(-\frac{j\pi}{4}\right)\right]}{2}$$
$$H_{2I}(f) = \frac{\left[\exp(-j4\pi f T_b) - \exp\left(-\frac{j\pi}{4}\right)\right]}{2} \tag{12}$$

respectively. In the Q interferometer, the lower branch has an excess phase shift of $-\pi/4$, so that the transfer functions to the sum and difference output ports are, respectively

$$H_{1Q}(f) = \frac{\left[\exp(-j4\pi f T_b) + \exp\left(\frac{j\pi}{4}\right)\right]}{2}$$
$$H_{2Q}(f) = \frac{\left[\exp(-j4\pi f T_b) - \exp\left(\frac{j\pi}{4}\right)\right]}{2}. \tag{13}$$

With appropriate coding, as described in [3], binary decisions on the sampled outputs of the I and Q branches yield, respectively, the first and second bits encoded in each symbol. Thus, each of the I and Q branches can be modeled as a separate 2-DPSK system, as described in Section II-A, with the modifications to the symbol duration MT_b, symbol stream I_n, and interferometer transfer functions described in this section. In order to compute the BER of the 4-DPSK system, we separately compute the BERs of each of these two 2-DPSK systems and then average the results. Note that CD, PMD, and optical bandpass filtering can lead to crosstalk between these two 2-DPSK systems. The impact of this crosstalk is accounted for in the BER calculation technique described in the following section.

III. Error Probability Computation

The BER calculation method employed in this paper was proposed by Forestieri [11] and is referred to here as the KLSE method. Although the technique was originally used to evaluate the BER in optically preamplified OOK systems with arbitrary pulse shape, optical/electrical filtering, and CD, it is applicable to DPSK systems, provided that the input electric field $x(t)$ can be expressed in the form (1) or, more generally, if its Fourier transform can be obtained. We observe that both PMD and a delay-line interferometer can be modeled in terms of generalized optical filters.

The essence of the KLSE method is as follows. The transmitted bit stream is assumed to be a periodic repetition of a binary de Bruijn sequence[2] [24], [25] such that the input signal electric field can be expanded in a Fourier series. The ASE noise is also expressed in a Fourier series using a Karhunen–Loeve expansion. With both the signal and noise expressed in this way, the decision sample can be readily expressed and will comprise three terms: signal, signal–ASE beat noise, and ASE–ASE beat noise. The original contribution of Foriestieri is to express all these terms in matrix form and, by using matrix transformation techniques, to combine both noises into one term. This term can be expressed, in general, as a noncentral quadratic form of Gaussian random variables and has a noncentral chi-square distribution. Thus, the moment-generating function (MGF) of the decision sample can be obtained, and the BER can be evaluated from it by using the inverse Laplace transform and saddle-point integration approximation. In the interest of brevity, we will not provide a mathematical description of the KLSE method; [11] provides all the details required to implement this technique.[3]

In order to compute the BER for a 2-DPSK system, referring to the two-PSP model shown in Fig. 3, we use the KLSE method to obtain the MGF of the decision variables in each subsystem. Because the ASE noises in the two PSPs are independent so are the decision variables in the two subsystems. Hence, to obtain the MGF of the combined decision sample, we simply multiply the MGFs of the two subsystems. In computing the BER for a 4-DPSK system, we use this technique to compute the BER for the I and Q signals separately and then average the two BERs.

We now make some observations about applying the KLSE method to DPSK systems.

- Unlike an OOK system, a DPSK system uses two photodetectors and, hence, the decision variables are given by the difference between two photocurrents (after low-pass filtering and sampling), both of which can be expressed as quadratic forms of Gaussian random variables. Because these two photocurrents are correlated, although the MGF of either one can be obtained readily, it is not straightforward to find the MGF of their difference. The easiest way to obtain the MGF of the decision variables is to combine corresponding terms in the two photocurrents (e.g., the two ASE–ASE noise terms) into one term before representing them in matrix form. This can be done because all the noise terms result from the same ASE. We then write down the combined decision variable in matrix form and, by using matrix transformations, express it in a noncentral quadratic form of Gaussian random variable, thereby obtaining its MGF.
- One must carefully choose the length of the de Bruijn sequence. In a 2-DPSK system, to take account of the ISI caused by CD, we need to consider all possible five-symbol patterns. As one bit is encoded into one symbol, a 2^5-b de Bruijn sequence is found to be adequate to achieve this goal.[4] In 4-DPSK system, however, as two bits are encoded into one symbol and there are four different symbols, if we considered all five-symbol patterns, we would need to use a 2^{10}-b de Bruijn sequence. As the computational complexity of the KLSE method is approximately proportional to the squared length of the de Bruijn sequence, it is difficult to use such a long sequence. Hence, in 4-DPSK systems, we generally consider shorter three-symbol patterns and use a 2^6-b de Bruijn sequence, which restricts us to studying weak-to-moderate CD effects (this approximation is valid for CD penalties of at least 2 dB). By contrast, three-symbol patterns are long enough for the study of PMD effects, because even strong PMD (e.g., $\Delta\tau = 1.6T_b$ for 4-DPSK) only causes ISI between immediately adjacent symbols.

TABLE I
BANDWIDTHS OF OPTICAL FILTER AND ELECTRICAL FILTER

	FP + Fifth-Order Bessel		FBG + Fifth-Order Bessel	
	B_o/R	B_e/R	B_o/R	B_e/R
NRZ-OOK	1.6	0.6	1.6	0.6
RZ-OOK	1.8	0.65	2.4	0.65
NRZ-2-DPSK	2.2	0.55	1.6	0.6
RZ-2-DPSK	2.2	0.65	2.2	0.65
NRZ-4-DPSK	1.6	0.275	1.1	0.275
RZ-4-DPSK	1.3	0.275	0.8	0.25

In order to justify the applicability of the KLSE method to DPSK systems, we compare the BERs of four DPSK systems computed using two distinct approaches: the KLSE method and Monte Carlo simulation [24]. These systems include NRZ-2-DPSK, NRZ-4-DPSK, RZ-2-DPSK, and RZ-4-DPSK. In all these systems, an FP optical bandpass filter and a fifth-order Bessel electrical low-pass filter are used. Filter bandwidths are selected following Table I, in which all the bandwidths have been chosen to minimize the BER when both CD and PMD are absent. When we compute the BER using the KLSE method, we use a 2^5-b de Bruijn sequence for 2-DPSK systems and a 2^6-b de Bruijn sequence for 4-DPSK systems. When we estimate BER with Monte Carlo simulation, for all systems we use pseudorandom bit sequence of length $2^{10} - 1$. Fig. 5 shows computed BERs as a function of E_b/N_0 when CD and PMD are absent. It is clear that the two approaches agree quite well in all cases, justifying the authors' use of the KLSE method for DPSK systems. As expected, it is also evident that, for a given BER, 2-DPSK requires a lower E_b/N_0 than 4-DPSK, while RZ-DPSK requires a lower E_b/N_0 than NRZ-DPSK.

The KLSE method can also be used to calculate the BER for a DPSK system using asynchronous heterodyne reception [18].

[2]A binary de Bruijn sequence is the *shortest circular* sequence of length 2^n such that every binary string of length n occurs exactly once. For example, an 8-b de Bruijn sequence is 01011100, which contains all the 3-b strings from 000 to 111, and can be used to account for ISI due to one bit on either side of the desired bit or the preceding two bits. A binary de Bruijn sequence of length 2^n can be produced by adding a 0 digit to a pseudorandom binary sequence of length $2^n - 1$ at the place where there are $n - 1$ zeros.

[3]Note there exists a typographical error in [11]: in (A.12) the indexes i and j should be swapped, i.e., $i - j$ is to be replaced by $j - i$, as is evident by comparing (A.9) with (A.10).

[4]In a 2-DPSK system, after differential coding, a 2^5-b de Bruijn bit sequence does not yield all possible five-symbol patterns, but we find that the patterns that are not produced make a negligible contribution to the BER. Similar results are observed for 4-DPSK systems.

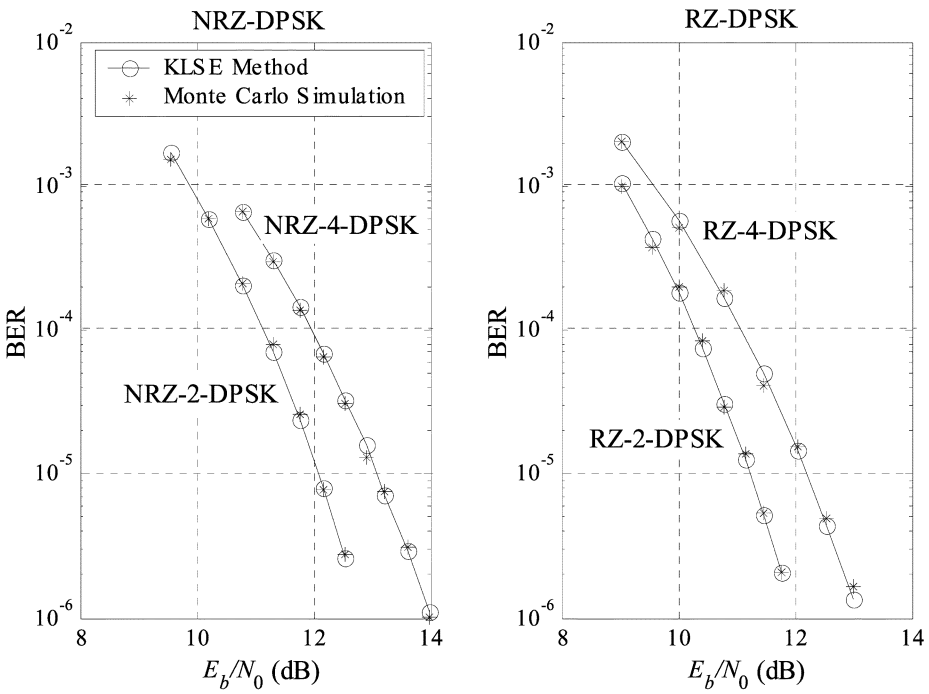

Fig. 5. Comparison of the BER versus E_b/N_0 obtained using the KLSE method and Monte Carlo simulation for binary and quaternary (a) NRZ-DPSK systems and (b) RZ-DPSK systems.

One simply needs to model the electrical delay-and-multiply demodulator used in the asynchronous heterodyne receiver as the "interferometer + square-law detector + subtractor" combination shown in Fig. 2, which performs an equivalent demodulating function and permits the KLSE method to be applied. Preamplified direct detection and heterodyne reception for DPSK have been proved to have identical performance under certain conditions [26] and, hence, it is not surprising that the analytical method designed for one scheme can be applied to the other.

IV. Dispersion Effects

In this section, we study the impact of CD and PMD on NRZ- and RZ-DPSK systems, using the KLSE method to compute the BER. In all cases, the system model is the "two-PSP" model shown in Fig. 3, which accounts for two polarizations of ASE noise. A bit rate of 10 Gb/s is assumed in all cases. The optical bandpass filter is either an FP filter or an FBG filter, while the electrical low-pass filter is always a fifth-order Bessel type. For each system type, the filter bandwidths have been selected to minimize the BER in the absence of CD and PMD and are indicated in Table I.[5] When CD or PMD is characterized in terms of penalties, these are the power penalties at 10^{-9} BER, which is the increase in energy per bit required to maintain this BER value when dispersion is present. Note that these power penalties can also be interpreted as optical signal-to-noise ratio (OSNR) penalties, since we consider the linear propagation regime. We also characterize PMD in terms of an outage probability criterion.

[5]We have also considered choosing the filter bandwidths to minimize the BER in the presence of moderate CD or PMD but have obtained values close to those in Table I.

For reference, the power penalties for OOK using NRZ and RZ formats caused by CD and PMD are also evaluated. In the case of OOK, the NRZ and RZ elementary pulse shapes are given by (2), and the KLSE method is used for the calculation of BER.

A. Chromatic Dispersion

In order to study the impact of CD alone, we neglect PMD by setting $\Delta\tau = 0$ in (11). Fig. 6 presents the 10^{-9} BER power penalty of NRZ- and RZ-OOK, 2-DPSK and 4-DPSK, versus the CD index $\zeta \equiv R^2LD$ in units of 10^4 $(\text{Gb/s})^2$ ps/nm. We assume $\lambda = 1.55$ μm. Note that because these signals are all chirp free, the behavior at positive and negative ζ is symmetrical, and it is sufficient to consider positive ζ. When either the NRZ or RZ format is used, CD causes smaller power penalties for 2-DPSK than for OOK, particularly when an FBG filter is used. Comparing the two 2-DPSK formats, RZ-2-DPSK and NRZ-2-DPSK exhibit similar penalties when the dispersion is weak [$\zeta < 6$ in Fig. 6(a) and $\zeta < 3$ in Fig. 6(b)]; however, for stronger CD, the power penalty of RZ-2-DPSK increases rapidly and becomes much larger than that of NRZ-2-DPSK. Similar observations can be made about the NRZ-OOK and RZ-OOK formats. Intuitively, this arises because the signal power spectrum has a wider main lobe for RZ than for NRZ.

4-DPSK, because its symbol rate is half the bit rate and its power spectrum is only half as wide as those of OOK or 2-DPSK, exhibits much smaller CD power penalties than the latter two modulation techniques. As shown in Fig. 6(a), when an FP optical filter is used, the power penalties for NRZ-4-DPSK are only about one fifth of those for NRZ-OOK and NRZ-2-DPSK. RZ-4-DPSK performs even better than NRZ-4-DPSK in combating CD. For example, when an FP

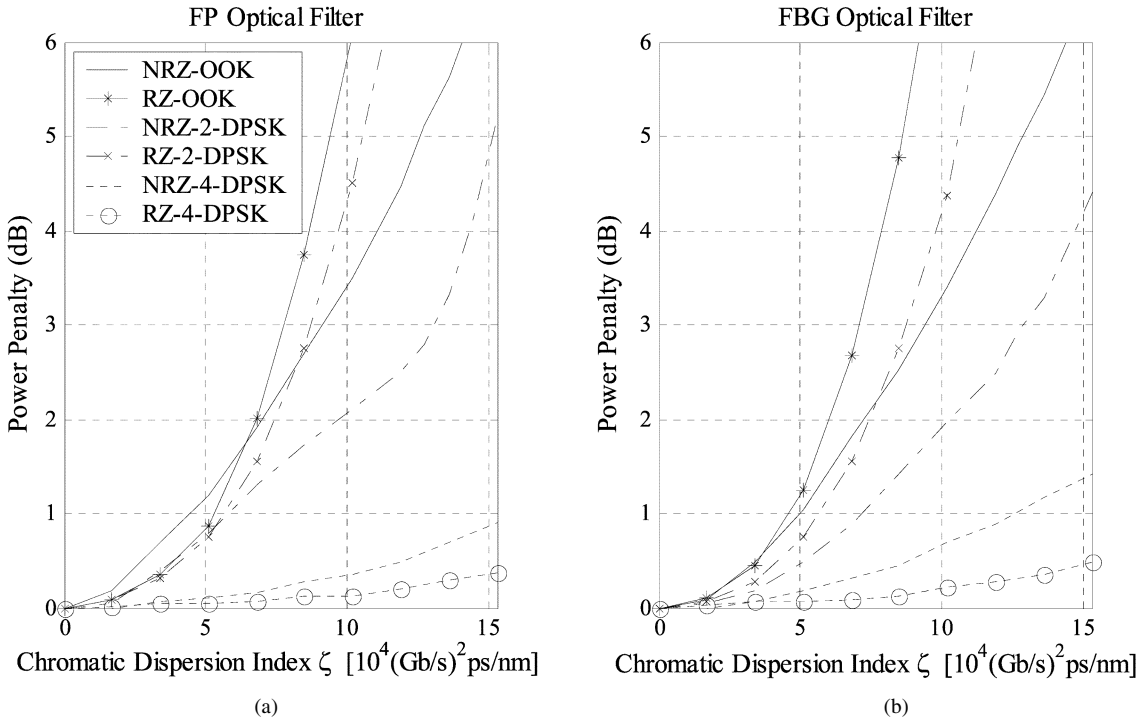

Fig. 6. Chromatic-dispersion-induced power penalty as a function of chromatic dispersion index ζ for NRZ- and RZ-OOK, 2-DPSK, and 4-DPSK systems with a fifth-order Bessel electrical filter and (a) FP optical filter or (b) FBG optical filter.

filter is used, the CD power penalty for RZ-4-DPSK is only one half that of NRZ-4-DPSK. This observation may seem counter-intuitive because in the cases of both 2-DPSK and OOK, RZ formats tend to be degraded more rapidly by CD than NRZ formats. If we examine Fig. 6(a) closely, we see that RZ-OOK has a smaller power penalty than NRZ-OOK for $\zeta < 6.5$, and RZ-2-DPSK has a smaller power penalty than NRZ-2-DPSK for $\zeta < 5$. For the range shown in the figure, $\zeta < 15$, 4-DPSK is in the weak-dispersion regime, so it is indeed plausible for RZ-4-DPSK to incur smaller power penalties than NRZ-4-DPSK in this regime. We found that for both FP and FBG filters, the penalties for RZ-4-DPSK and NRZ-4-DPSK cross at $\zeta \approx 32$,[6] beyond which RZ-4-DPSK has larger penalties than NRZ-4-DPSK. While it is difficult to explain intuitively why the crossover occurs at much larger values of ζ for 4-DPSK than for 2-DPSK or OOK, we observe that CD affects not only signal amplitude but also signal phase, and 4-DPSK is more sensitive to phase variations than either 2-DPSK or OOK.

It is useful to compare the CD tolerance of the different modulation schemes for a fixed power penalty of 1 dB. Assuming an FBG optical filter is used, the values of ζ corresponding to a 1-dB power penalty for NRZ-OOK, RZ-OOK, NRZ-2-DPSK, RZ-2-DPSK, NRZ-4-DPSK and RZ-4-DPSK are 5.0, 4.5, 7.2, 5.8, 12.5, and 19.6 respectively. At a bit rate of 10 Gb/s, these values of ζ correspond to transmission distances of 29, 26, 42, 34, 74, and 115 km, respectively, assuming $D(\lambda) = 17$ ps/nm/km. For a fixed power penalty of 2 dB, the corresponding values of ζ are 7.2, 6.0, 10.3, 7.3, 19.9, and 26.4, corresponding to transmission distances of 42, 35, 61, 43, 117, and 155 km. Note some of the values of ζ quoted above for 4-DPSK are larger than those appearing in Fig. 6.

Comparing the eye-penalty plots in [7] (not shown in this paper) with Fig. 6, we find the eye-penalty criterion accurately estimates CD power penalties for NRZ-2-DPSK only when the CD is severe ($\zeta > 12$). When the CD is not severe, the eye-penalty criterion underestimates the power penalty significantly and should not be relied upon.

B. Polarization-Mode Dispersion (PMD)

In order to observe the impact of first-order PMD clearly, we neglect CD by setting $\beta_2 = 0$ in (11). Fig. 7 shows the 10^{-9} BER power penalty of NRZ- and RZ-OOK, 2-DPSK and 4-DPSK, versus the ratio of DGD to bit duration $\Delta\tau/T_b$. We assume the worst-case value of the power splitting between the two PSPs, i.e., $\gamma = 0.5$ in (11). Comparing Fig. 7(a) with (b), we see that the relative robustness of different modulation schemes to PMD is largely independent of whether the optical filter is chosen to be of FP or FBG type. Because all five modulation schemes exhibit slightly smaller PMD penalties with FBG filters, we focus on the FBG case in the following discussion.

As seen in Fig. 7(b), NRZ-2-DPSK is slightly superior to NRZ-OOK in terms of PMD tolerance, as it exhibits about 10% lower PMD power penalties for strong PMD. For weak PMD, the ratio between the two power penalties is close to unity. A similar relationship exists between RZ-2-DPSK and RZ-OOK. 4-DPSK is much more resistant to PMD than either 2-DPSK or OOK. For example, NRZ-4-DPSK exhibits a PMD power penalty of only about one quarter that of NRZ-2-DPSK or NRZ-OOK in the case of weak PMD. This is to be expected, because in NRZ-4-DPSK, the symbol duration is twice as long as for the other two modulation schemes. RZ-DPSK, as it uses

[6]At these large values of ζ, the CD penalty is about 3 dB, and we perform computations using a 2^8-b de Bruijn sequence.

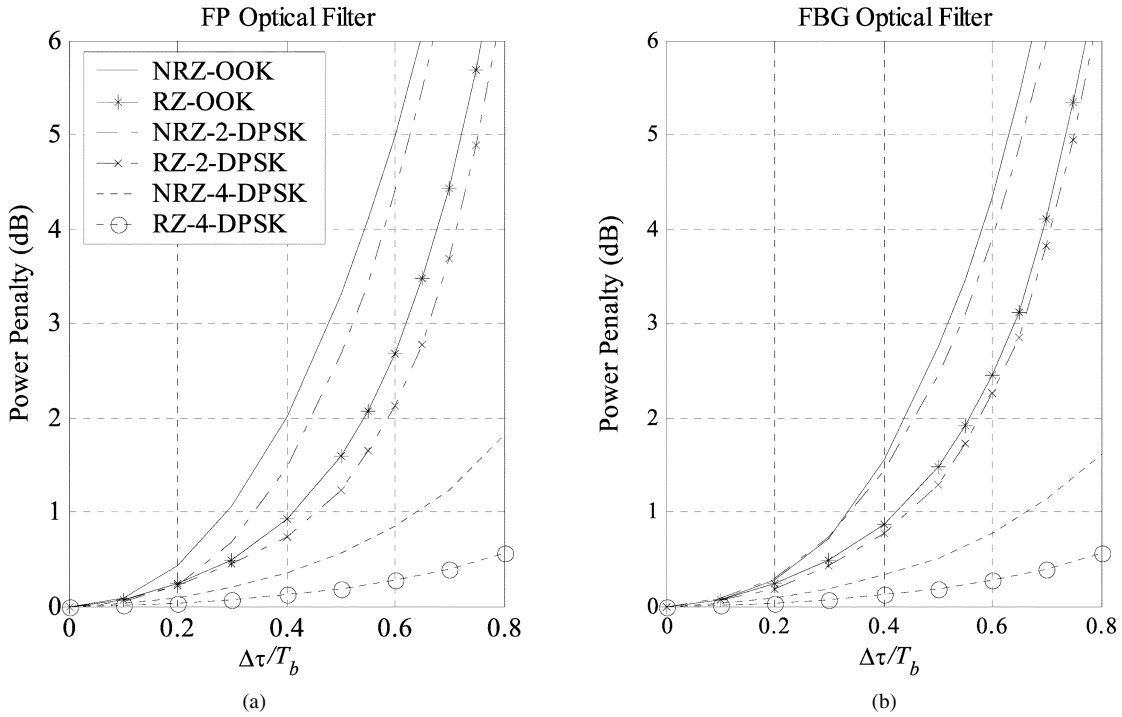

Fig. 7. PMD-induced power penalty as a function of DGD/bit duration ratio $\langle \Delta\tau \rangle / T_b$ for NRZ- and RZ-OOK, 2-DPSK, and 4-DPSK systems, with a fifth-order Bessel electrical filter and (a) FP optical filter or (b) FBG optical filter. The worst-case power-splitting ratio of polarization-mode dispersion is assumed, i.e., $\gamma = 0.5$.

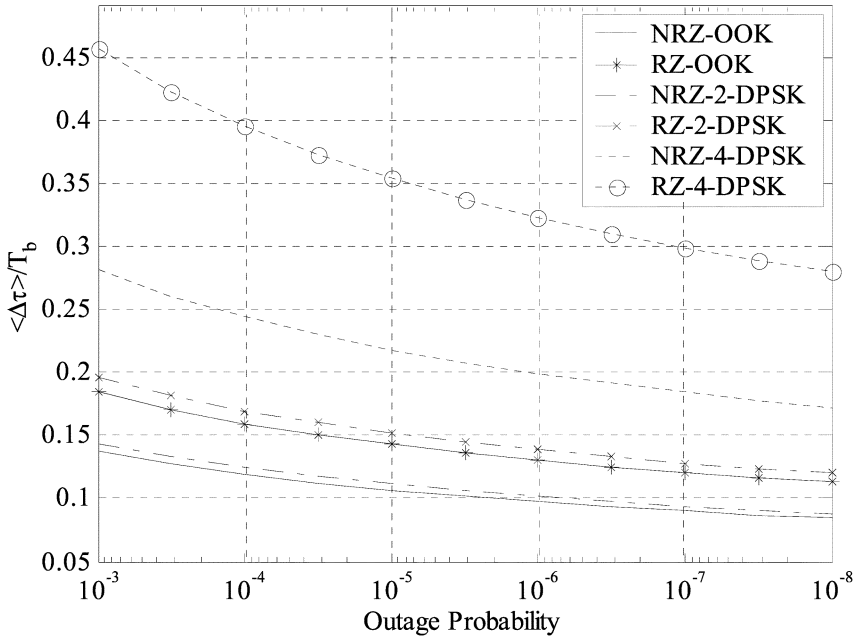

Fig. 8. Maximum allowable ratio of mean DGD to bit duration $\langle \Delta\tau \rangle / T_b$ as a function of outage probability, for NRZ- and RZ-OOK, 2-DPSK, and 4-DPSK systems, with a fifth-order Bessel electrical filter and a FBG optical filter.

a shorter pulse duration, exhibits much greater PMD tolerance than its NRZ counterparts (RZ-2-DPSK versus NRZ-2-DPSK and RZ-4-DPSK versus NRZ-4-DPSK).

For small power penalties ε, given in decibels, the first-order PMD impairment can be expressed as [21]

$$\varepsilon = A \left(\frac{\Delta\tau}{MT_b} \right)^2 \gamma(1-\gamma) \tag{14}$$

where, as in Section II, MT_b is the symbol duration. Recall that $M = 1$ for 2-DPSK and $M = 2$ for 4-DPSK. Using the power penalty data shown in Fig. 7(b), for NRZ-OOK, RZ-OOK, NRZ-2-DPSK, RZ-2-DPSK, NRZ-4-DPSK, and RZ-4-DPSK using an FBG filter, the parameter A is found to be about 39, 22, 36, 19, 37 and 14, respectively. Although the values of A are similar for NRZ-2-DPSK and NRZ-4-DPSK, the latter modulation scheme is much more tolerant to PMD, because the

symbol duration is twice as long. A similar comparison can be made between RZ-2-DPSK and RZ-4-DPSK.

In view of the statistical nature of PMD, instead of plotting the power penalty versus DGD, a better way to characterize PMD tolerance is by plotting the maximum allowable mean DGD versus outage probability, which is the probability for the power penalty to exceed N dB. To achieve this, we combine (14) with the Maxwellian PMD statistics and obtain a closed-form expression for the outage probability P_{out}. From the expression for P_{out}, the requirement for the maximum allowable mean DGD $\langle \Delta\tau \rangle$ of the fiber can be expressed as [22]

$$\frac{\langle \Delta\tau \rangle}{T_b} = \frac{4M\sqrt{N}}{\sqrt{\pi A \ln\left(\frac{1}{P_{\text{out}}}\right)}}. \tag{15}$$

Substituting values of the parameter A given above and assuming $N = 1$ dB, the maximum allowable values of the ratio $\langle \Delta\tau \rangle / T_b$ can be calculated and are shown as a function of outage probability P_{out} in Fig. 8. We see that when either the NRZ or RZ format is used, 2-DPSK can tolerate a slightly larger value of $\langle \Delta\tau \rangle / T_b$ than OOK. For NRZ-4-DPSK, the maximum allowable value of $\langle \Delta\tau \rangle / T_b$ is nearly twice of that for NRZ-2-DPSK or NRZ-OOK, which is to be expected because NRZ-4-DPSK has a symbol duration twice as long as the other two. The PMD tolerance of RZ-2-DPSK and RZ-4-DPSK greatly exceed their NRZ counterparts, because the RZ modulation schemes use shorter pulse durations. For example, at 10^{-5} outage probability, the maximum allowable value of $\langle \Delta\tau \rangle / T_b$ for RZ-2-DPSK is 1.4 times of that for NRZ-2-DPSK, and the maximum allowable value of $\langle \Delta\tau \rangle / T_b$ for RZ-4-DPSK is about 1.6 times of that for NRZ-4-DPSK (similar ratios are found at other values of the outage probability).

V. Conclusion

In this paper, we have applied the BER calculation method introduced by Forestieri for OOK systems to the case of DPSK systems using optical preamplifiers, interferometric demodulation, and direct detection. We have shown that if properly applied, this KLSE method accurately predicts the BER performance of these DPSK systems, and we have verified its accuracy using Monte Carlo simulations. Using the KLSE method, we have evaluated power penalties caused by CD and first-order PMD with 2-DPSK and 4-DPSK using NRZ and RZ formats, comparing these with OOK. We have found that 2-DPSK exhibits less power penalties than OOK in the presence of CD and the first-order PMD. NRZ-4-DPSK, as it has twice the symbol duration of these other techniques for a given bit rate, incurs CD and PMD power penalties of only about 1/4 $\sim$ 1/3 as large as NRZ-2-DPSK. RZ-2-DPSK, as compared with NRZ-2-DPSK, incurs smaller penalties due to PMD, but offers no advantage in terms of CD. RZ-4-DPSK offers CD and PMD penalties significantly smaller than all other techniques.

References

[1] M. Rohde, C. Caspar, N. Heimes, M. Konitzer, E.-J. Bachus, and N. Hanik, "Robustness of DPSK direct detection transmission format in standard fiber WDM systems," *Electron. Lett.*, vol. 36, pp. 1483–1484, Aug. 1999.

[2] H. Nizhizawa, Y. Yamada, Y. Shibata, and K. Habara, "10-Gb/s optical DPSK packet receiver proof against large power fluctuation," *IEEE Photon. Technol. Lett.*, vol. 11, pp. 733–735, June 1999.

[3] R. A. Griffin and A. C. Carter, "Optical differential quadrature phase-shift key (oDQPSK) for high capacity optical transmission," in *Tech. Dig. OFC 2002*, Washington, DC, pp. 367–368.

[4] A. H. Gnauck, G. Raybon, S. Chandrasekhar, J. Leuthold, C. Doerr, L. Stulz, A. Agarwal, S. Banerjee, D. Grosz, S. Hunsche, A. Kung, A. Marhelyuk, D. Maywar, M. Movagassaghi, X. Liu, C. Xu, X. Wei, and D. M. Gill, "2.5 Tb/s (64 × 42.7 Gb/s) transmission over 40 × 100 km NZDSF using RZ-DPSK format and all-Raman-amplified spans," in *Tech. Dig. Postdeadline Papers, OFC*, 2002, pp. FC2.1–FC2.3.

[5] W. Christoph, L. Jochen, and R. Werner, "RZ-DQPSK format with high spectral efficiency and high robustness toward fiber nonlinearities," presented at the ECOC, Copenhagen, Denmark, Sept. 2002, Paper 9.6.6.

[6] H. Bissessur, G. Charlet, E. Gohin, C. Simonneau, L. Pierre, and W. Idler, "1.6 Tb/s (40 × 40 Gb/s) DPSK transmission with direct detection," presented at the ECOC, Copenhagen, Denmark, Sept. 2002, Paper 8.1.2.

[7] A. F. Elrefale, R. E. Wagner, D. A. Atlas, and D. G. Daut, "Chromatic dispersion limitations in coherent lightwave transmission systems," *J. Lightwave Technol.*, vol. 5, pp. 704–709, May 1988.

[8] C. De Angelis, A. Galtarossa, C. Campanile, and F. Matera, "Performance evaluation of ASK and DPSK optical coherent systems affected by chromatic dispersion and polarization mode dispersion," *J. Opt. Commun.*, vol. 16, pp. 173–178, May 1995.

[9] G. Jacobsen, "Performance of DPSK and CPFSK systems with significant post-detection filtering," *J. Lightwave Technol.*, vol. 11, pp. 1622–1631, Oct. 1993.

[10] S. R. Chinn, D. M. Boroson, and J. C. Livas, "Sensitivity of optically preamplified DPSK receivers with Fabry–Perot filters," *J. Lightwave Technol.*, vol. 14, pp. 370–375, Mar. 1996.

[11] E. Forestieri, "Evaluating the error probability in lightwave systems with chromatic dispersion, arbitrary pulse shape and pre-and postdetection filtering," *J. Lightwave Technol.*, vol. 18, pp. 1493–1503, Nov. 2000.

[12] M. Kac and A. J. F. Siegert, "On the theory of noise in radio receivers with square law detectors," *J. Appl. Phys.*, vol. 18, pp. 383–397, 1947.

[13] J. E. Mazo and J. Salz, "Probability of error for quadratic detectors," *Bell Syst. Tech. J.*, vol. 44, pp. 2165–2186, 1965.

[14] J. Lee and C. Shim, "Bit-error-rate analysis of optically preamplified receivers using an eigenfunction expansion method in optical frequency domain," *J. Lightwave Technol.*, vol. 12, pp. 1224–1229, July 1994.

[15] G. Bosco, A. Carena, V. Curri, R. Gaudino, P. Poggiolini, and S. Benedetto, "A novel analytical method for the BER evaluation in optical systems affected by parametric gain," *IEEE Photon. Technol. Lett.*, vol. 12, pp. 152–154, Feb. 2000.

[16] P. J. Winzer, S. Chandrasekhar, and H. Kim, "Impact of filtering on RZ-DPSK reception," *IEEE Photon. Technol. Lett.*, vol. 15, pp. 840–842, June 2003.

[17] P. J. Winzer, M. Pfennigbauer, M. M. Strasser, and W. R. Leeb, "Optimum filter bandwidths for optically preamplified NRZ receivers," *J. Lightwave Technol.*, vol. 19, pp. 1263–1273, 2001.

[18] G. P. Agrawal, *Fiber-Optic Communication Systems*. New York: Wiley, 2002.

[19] D. E. Johnson, J. R. Johnson, and H. P. Moore, *A Handbook of Active Filters*. Englewood Cliffs, NJ: Prentice-Hall, 1980.

[20] C. D. Poole and R. E. Wagner, "Phenomenological approach to polarization dispersion in long single-mode fibers," *Electron. Lett.*, vol. 22, pp. 1029–1030, Sept. 1986.

[21] C. D. Poole and C. R. Giles, "Polarization-dependent pulse compression and broadening due to polarization dispersion in dispersion-shifted fiber," *Opt. Lett.*, vol. 13, pp. 155–157, Feb. 1988.

[22] H. Kolgelnik, R. M. Jopson, and L. E. Nelson, "Polarization-mode dispersion," in *Optical Fiber Telecommunication IVB Systems and Impairments*, I. P.Ivan P. Kaminow and T.Tingye Li, Eds. San Diego, CA: Academic Press, 2002, pp. 725–861.

[23] A. O. Lima, I. T. Lima, T. Adali, and C. R. Menyuk, "Comparison of power penalties due to first- and all-order PMD distortions," presented at the ECOC, Copenhagen, Denmark, Sept. 2002, Paper 7.1.2.

[24] M. C. Jeruchim, P. Balaban, and K. S. Shanmugan, *Simulation of Communication Systems*. New York: Plenum Press, 1992, pp. 496–503.

[25] S. Golomb, *Shift Register Sequences*. Laguna Hills, CA: Aegean Press, 1982.

[26] O. K. Tonguz and R. E. Wagner, "Equivalence between preamplified direct detection and heterodyne receivers," *IEEE Photon. Technol. Lett.*, vol. 3, pp. 835–837.

[27] G. J. Foschini and C. D. Poole, "Statistical theory of PMD in single mode fibers," *J. Lightwave Technol.*, vol. 9, pp. 1439–1456, Nov. 1991.

Jin Wang (S'03) was born in Hubei, China, in 1975. He received the B.S. and M.E. degrees in electronics from Peking University, Peking, China, in 1996 and 1999, respectively. He is currently pursuing the Ph.D. degree at the University of California, Berkeley.

His main research interest is the performance evaluation of long-haul fiber-optic communication systems.

Joseph M. Kahn (F'00) received the A.B., M.A., and Ph.D. degrees in physics from the University of California, Berkeley, in 1981, 1983, and 1986, respectively.

From 1987 to 1990, he was at AT&T Bell Laboratories, Crawford Hill Laboratory, Holmdel, NJ. He demonstrated multi-gigabits-per-second coherent optical fiber transmission systems, setting world records for receiver sensitivity. From 1990 to 2003, he was on the faculty of the Department of Electrical Engineering and Computer Sciences at the University of California, Berkeley, performing research on optical and wireless communications. Since 2003, he has been a Professor of Electrical Engineering at Stanford University, Stanford, CA. His current research interests include single- and multi-mode optical fiber communications, free-space optical communications, and microelectromechanical systems (MEMS) for optical communications.

Prof. Kahn received the National Science Foundation Presidential Young Investigator Award in 1991. From 1993 to 2000, he served as a Technical Editor of *IEEE Personal Communications Magazine*.